IOP Publishing Biomed. Mater. 20 (2025) 025024 https://doi.org/10.1088/1748-605X/adae48

Biomedical Materials

PAPER

RECEIVED
5 September 2024

REVISED
17 January 2025

ACCEPTED FOR PUBLICATION
24 January 2025

PUBLISHED
13 February 2025

Chitosan and ibuprofen grafted electrospun polylactic acid/gelatin membrane mitigates inflammatory response

Qiaolin Ma[1,6], Anlin Yin[2,6], Xinjian Wan[3], Binbin Sun[1], Hongsheng Wang[1], Mohamed El-Newehy[4], Meera Moydeen Abdulhameed[4], Xiumei Mo[1], Jinglei Wu[1,*] and Tian Tu[5,*]

[1] Shanghai Engineering Research Center of Nano-Biomaterials and Regenerative Medicine, College of Biological Science and Medical Engineering, Donghua University, Shanghai 201620, People's Republic of China
[2] College of Material and Textile Engineering, Jiaxing University, Jiaxing 314001, People's Republic of China
[3] Digestive Endoscopic Center, Shanghai Sixth People's Hospital Affiliated to Shanghai Jiao Tong University School of Medicine, Shanghai 200233, People's Republic of China
[4] Department of Chemistry, College of Science, King Saud University, PO Box 2455, Riyadh 11451, Saudi Arabia
[5] Plastic and Aesthetic Center, The First Affiliated Hospital, Zhejiang University School of Medicine. 79 Qingchun Road, Hangzhou 310003, People's Republic of China
[6] These authors contributed equally to this study.
[*] Authors to whom any correspondence should be addressed.

E-mail: jw@dhu.edu.cn and tutian1993sjt@zju.edu.cn

Keywords: electrospun membrane, anti-inflammatory, antibacterial, macrophage polarization

Supplementary material for this article is available online

Abstract

Electrospun membranes with biomimetic fibrous structures and high specific surfaces benefit cell proliferation and tissue regeneration but are prone to cause chronic inflammation and foreign body response. To solve these problems, we herein report an approach to functionalize electrospun membranes with antibacterial and anti-inflammatory components to modulate inflammatory responses and improve implantation outcomes. Specifically, electrospun polylactic acid (PLA)/gelatin (Gel) fibers were grafted with chitosan (CS) and ibuprofen (IBU) via carbodiimide chemistry. Our results show that the surface modification strategy endows electrospun membranes with moderate antibacterial activities and sustained release of anti-inflammatory drugs. The electrospun PLA/Gel-CS-IBU membrane showed good antioxidant and anti-inflammatory activity as evidenced by suppressing M1 polarization and promoting M2 polarization of macrophages *in vitro*. Similarly, it induced significantly milder chronic inflammatory responses *in vivo* than unmodified electrospun membranes. Given the good anti-inflammatory and antibacterial effects, this strategy might improve the biological performance of electrospun membranes as implants in clinics.

1. Introduction

Electrospun membranes have been widely used in tissue engineering and regenerative medicine applications [1–5]. Electrospun fibers provide physical support for cells and tissues and morphologically mimic extracellular matrix, which provide topological signals required for tissue regeneration [6–9]. The use of natural protein molecules as raw materials for electrospinning is challenging [8, 10–13]. Natural proteins, such as oilseed proteins, typically have a spherical structure, low viscosity in protein solutions, short molecular chains, and lack of intermolecular entanglement. In addition, electrospun membranes based on natural protein molecules have poor extensibility. There are currently various materials used to prepare biodegradable electrospun fibers, including polylactic acid (PLA), polycaprolactone (PCL), polyglycolide acid (PGA), and other polyester compounds. However, the foreign body response (FBR) and degradation-mediated aseptic inflammation after materials implantation are inevitable [14–16]. These adverse reactions can impair tissue regeneration and limit the application of electrospun

materials. Thus, current research is focused on finding ways to mitigate the negative effects of electrospun fibers.

Macrophage activation is a crucial event in initiating the FBR to implants [17–19]. It plays an important role in the activation of adaptive immune system through phagocytosis and secretion of various cytokines and growth factors. They are activated to different phenotypes in response to various stimuli. However, the switch in their phenotypic function is typically temporal. After the implantation of electrospun membranes, macrophages temporally polarize into pro-inflammatory macrophages (M1) and anti-inflammatory macrophages (M2) in turn [18, 20–22]. M1 macrophages are a type of immune cells that participate in the immune response by secreting pro-inflammatory cytokines and chemokines, and produce reactive oxygen species (ROSs) and nitric oxide [23]. The aggregation and presence of M1 macrophages can lead to chronic inflammation and tissue fibrosis, ultimately leading to a bad outcome [24, 25]. Conversely, when M2 macrophages appear and aggregate, it indicates that inflammation is decreasing, promoting tissue regeneration and wound healing, which is a favorable process. The initial phenotypic transition of macrophages from M1 to M2 promotes strong integration and beneficial remodeling of biomaterials with the host tissue [26, 27]. Therefore, modifying the surface of electrospun fibers rationally to induce M1-to-M2 phenotypic transition in macrophages at an early stage is a viable approach to reduce their FBR. Previous studies demonstrated that slow release of nonsteroidal anti-inflammatory drugs (NSAIDs) in tissues accelerates desirable phenotypic switching processes and attenuates macrophage-mediated FBR and host-anti-graft response [28]. In previous studies, chitosan (CS) was used as a linking agent to graft the small molecule anti-inflammatory drug itaconic acid (OI) onto electrospun nanofibers [29]. The nanofiber membrane grafted with OI showed great anti-inflammatory activity and effective regulation of inflammatory response in diabetic wound models. In addition, we recently reported that a CS-ibuprofen (CS-IBU) conjugate by carbodiimide chemistry and further modified it with methacrylic anhydride to obtain a photocrosslinkable hydrogel with anti-inflammatory capacity [30]. These studies highlight the potential of CS-drug conjugates for biomaterial functionalization. Therefore, we propose that NSAIDs can be loaded onto the surface of the electrospun membranes through covalently bonded connections and then locally released so that macrophages can be recruited to the tissue periphery and be induced into an M2 functional phenotype, which will attenuate the tissue FBR.

This study aims to modulate the foreign body reaction and inflammation levels of electrospun membranes after implantation. Polylactic acid, due to its biodegradability, biocompatibility, and excellent mechanical properties, have been widely used to prepare electrospun nanofiber membranes [31, 32]. Gelatin, a natural biopolymer, is frequently used to blended with synthetic polymers to reduce their hydrophobicity and promote biological performance of electrospun fibers [33]. We grafted ibuprofen (IBU) on the surface of polylactic acid (PLA)/gelatin (Gel) electrospun membrane using chitosan (CS) as a linker. We investigated the modulatory effect of electrospun membranes on macrophage polarization *in vitro* and inflammatory response in a subcutaneous implantation model of mice.

2. Materials and methods

2.1. Materials

Poly-L-lactic acid (PLLA, Mw 110 000, hereafter referred to as PLA) was purchased from Rhawn Chemicals Co., Ltd type A gelatin from porcine skin was purchased from Sigma-Aldrich. 1,1,1,3,3,3-hexafluoro-2-propanol (HFIP) was purchased from Shanghai Da-Rui Fine Chemical Co., Ltd (Shanghai, China). Chitosan (90% deacetylation degree, 200 kDa), IBU and 2-(N-morpholino) ethanesulfonic acid (MES) were obtained from Macklin Biochemical Co., Ltd (Shanghai, China). 1-ethyl-3-(3-dimethylaminopropyl) carbodiimide (EDC) was obtained from Sinopharm Chemical Reagent Co., Ltd (Shanghai, China). Hydrochloride (HCl) and N-hydroxysuccinimide (NHS) were provided by Adamas Reagent Ltd, Shanghai. Luria-Bertain (LB) Broth and LB Broth Agar were provided by Sangon Biotech (Shanghai, China).

2.2. Preparation of electrospun membranes

PLA and gelatin were dissolved in HFIP with a PLA/gelatin ratio of 8:2 (w/w) at a concentration of 12% (w/v). The PLA/ gelatin solution was fed at a speed of 1.2 ml h^{-1} under a charge of 12 kV high voltage to generate fibers at room temperature with a humidity ranging from 50% to 70%. A PLA/Gel membrane (10 cm × 15 cm, ∼200 μm thickness) was obtained by collecting electrospun fibers on a slow-speed mandrel (6 cm diameter, 120 rpm) at 10 cm.

Chitosan (5 mM repeat unit) was dissolved in 0.1 M HCl solution at 1% concentration and stirred at room temperature. Subsequently, EDC (2.5 mM), NHS (1 mM), and ibuprofen (0.5 mM) were dissolved in ethanol solution and slowly added to CS solution, stirring at room temperature until the solution became transparent. The reaction was maintained at room temperature for 6 h in a dark environment and

poured into a glass dish for air drying, then washed with ethanol 3 times, and finally air dried to obtain the CS-IBU conjugate.

To obtain PLA/Gel-CS-IBU membrane, electrospun PLA/Gel membrane (10 cm × 10 cm) was soaked in 100 ml CS-IBU aqueous solution (1 mg ml^{-1}) for 12 h, and then the sample dried at room temperature. After that, the sample was soaked in MES buffer solution and cross-linked with EDC/NHS at room temperature for 24 h, followed by thorough wash with deionized water 6 times. The obtain PLA/Gel-CS-IBU membrane was dried at room temperature for further use.

2.3. Characterization of electrospun membranes

Electrospun membranes were sputter-coated with gold, and the surface morphology of electrospun membranes was observed by Phenom XL desktop scanning electron microscopy (SEM) (Phenom, Netherlands) under 5 kV acceleration voltage. For each electrospun membrane, 100 fibers were randomly selected from SEM images and measured the fiber diameter of membranes by Image J. The chemical structure of the electrospun membranes was characterized by Nicolet-760 FITR spectrometer at the wavelength range of 4000–400 cm^{-1}.

Membranes were cut into 10 mm × 40 mm strip specimens along the fiber arrangement direction for uniaxial tensile test. The samples were soaked in PBS for 24 h and stretched at 10 mm min^{-1} using a universal testing machine (Instron 5567, Norwood, MA) equipped with a 50 N load cell until failure. Before starting the experiment, the upper and lower ends of the sample were clamped by 1 cm each and straightened them, the length of the straightening was measured and recorded. The ultimate tensile strength (UTS) was expressed as the maximum tensile strength before failure and Young's modulus was calculated as the slope of the initial linear portion of the stress–strain curve ($n = 8$).

To evaluate the *in vitro* degradation, membranes were cut into 1 cm × 1 cm squares and weighed (m_0), soaked in PBS, and incubated in PBS at 37 °C. At pre-determined time points, samples were removed, washed with deionized water 3 times, freeze-dried, and weighed (m_1) ($n = 3$). The weight loss of samples was calculated as the following formula:

$$\text{weight loss } (\%) = \left[\frac{m_1 - m_0}{m_0}\right] \times 100.$$

The drug release of IBU was analyzed by UV–vis spectrophotometry. PLA/Gel-CS-IBU membrane was cut into 1 cm × 1 cm squares, weighed, soaked in 5 ml PBS, and statically incubated at 37 °C. At the predetermined time, the absorbance of IBU was measured at 222 nm with 1 ml of solution by UV–vis spectrophotometer, and an equal volume of PBS was added to continue incubation ($n = 3$). The cumulative concentration of IBU was calculated according to the standard curve.

2.4. Antibacterial properties of membranes

The antibacterial properties of PLA/Gel-CS-IBU membrane were evaluated by *E. coli* and *S. aureus*. Membranes were prepared into 11 mm discs and irradiated under ultraviolet light overnight. Bacteria were incubated in LB broth medium and incubated at 100 rpm at 37 °C overnight. Each sample was inoculated with 100 μl bacterial inoculum solution (10^5 CFU ml^{-1}) and incubated at 37 °C overnight. After incubation, the inoculating solution was stirred in sterile PBS for 10 min, continuously diluted, and then 100 μl diluted inoculum solution was drawn and spread on LB Agar plates. After incubation at 37 °C for 24 h, bacterial colonies were imaged using an automated colony counter (Shineso Science & Technology Co., Ltd, Hangzhou) and counted by Image J ($n = 3$).

2.5. Cytocompatibility assessment

Cytocompatibility assessment was conducted by incubating electrospun membranes with murine macrophages. RAW 264.7 macrophage cell line was provided by the Stem Cell Bank of Chinese Academy of Sciences (Shanghai) and cultured in high glucose Dulbecco's Modified Eagle Medium (Hyclone) supplemented with 10% fetal bovine serum, 1% penicillin/streptomycin. Cells were cultured in a 37 °C incubator containing 5% CO_2. Membranes were punched into 11 mm discs and placed in the 48-well plate, irradiated under UV for 12 h, and soaked in 70% ethanol for 1 h. Membranes were washed with PBS to remove the debris, added appropriate medium, and incubated for 12 h. Macrophages were seeded on membranes at a density of 5 × 10^5 cells per well, and incubated in a 37 °C incubator with 5% CO_2. The proliferation of macrophages was detected by a CCK-8 assay. Macrophages were stained with Calcein-AM and propyl iodide, and then live/dead images were collected by a DMi 8 inverted fluorescence microscopy (Leica, Germany). Finally, macrophages cultured on membranes were fixed with 4% paraformaldehyde, gradient dehydrated with ethanol, and dried at room temperature. The morphology of macrophages on membranes was observed by SEM (Phenom, Netherlands).

2.6. Anti-inflammatory activity assessment *in vitro*

The effect of electrospun membranes on the polarization of macrophages was studied by simulating the inflammatory environment *in vitro*. Membranes were prepared into discs with a diameter of 35 mm, then disinfected under ultraviolet irradiation and placed in 6-well plates. Macrophages were seeded on membranes at a density of 3.0 × 10^5 cells per well. After

Table 1. Primer sequences of genes for qRT-PCR analysis.

Gene names	Primer sequence (5′–3′)
CD86	F: 5′ GAGCACTATTTGGGCACAGAGAAAC 3′ R: 5′ TGAAGTCGTAGAGTCCAGTTGTTCC 3’
CD163	F: 5′ CCTCCTCATTGTCTTCCTCCTGTG 3′ R: 5′ CATCCGCCTTTGAATCCATCTCTTG 3’
IL-1β	F: 5′ CTCGCAGCAGCACATCAACAAG 3′ R: 5′ CCACGGGAAAGACACAGGTAGC 3’
IL-6	F: 5′ TTCTTGGGACTGATGCTGGTGAC 3′ R: 5′ GTGGTATCCTCTGTGAGGTCTCCTC 3’
IL-4	F: 5′ GTTGTCATCCTGCTCTTCTTTCTCG 3′ R: 5′ CATGGCGGTCCCTTCTCCTGTG 3’
IL-10	F: 5′ GGTTGCCAAGCCTTATCGGAAATG 3′ R: 5′ GCCGCATCCTGAGGGTCTTC 3’
GADPH	F: 5′ AGAAGGTGGTGAAGCAGGCATC 3′ R: 5′ CGAAGGTGGAAGAGTGGGAGTTG 3’

macrophages adhered to the membranes, the positive control group and experimental groups were respectively added with 1 ml 100 ng ml^{-1} lipopolysaccharide (LPS, TargetedMol) per well to induce the polarization of macrophages for 8 h. Membranes were washed gently with PBS three times to remove residual LPS, and added complete culture medium. After 24 h culture, CD86 and CD206 antibodies (Biolegend) were added to bind with macrophages. The expressions of CD86 and CD206 were detected by CytoFLEX flow cytometry system (Beckman Coulter).

Following the same procedure as described above, macrophages were stained with 2′,7′-dichlorodihydrofluorescein diacetate (DCFH-DA) probe for 30 min and incubated with DAPI for 15 min ($n = 3$). The levels of ROS in macrophages were detected by a fluorescence microscope (DMi 8, Leica, Germany) and flow cytometry. The level of NO was detected by a nitric oxide kit (Beyotime Biotechnology Inc., Shanghai, China). Macrophages were implanted on membranes at a density of 5.0×10^5 cells per well and cultured according to the same procedure described above. The absorbance of the cell culture medium at 540 nm was detected by a microplate reader (Multiskan MK3, Thermo, USA), and the concentration of NO was calculated according to the standard curve.

2.7. *In vivo* assessments

Membranes were subcutaneously implanted into male C57BL/6 mice (6 weeks old) to evaluate the biocompatibility. Animals were purchased from Hangzhou Medical College and then kept in an SPF environment without hindrance to reach food and water.

This animal study was approved by the Animal Experimental Ethical Committee of the First Affiliated Hospital, Zhejiang University School of Medicine—approval: 2024–432. Briefly, membranes were punched into a disc-shaped sample with a diameter of 11 mm and immersed in 70% ethanol for 30 min for disinfection, followed by UV irradiation for 24 h. Then mice were anesthetized by inhalation of 4.5% isoflurane for induction and then 1.5% isoflurane for maintenance. Under aseptic conditions, two 1.5 cm incisions were made longitudinally on the bilateral dorsal skin for subcutaneous pocket creation. The subcutaneous pockets on a single mouse were implanted with membranes of the same group. After properly spreading, membranes were fixed on the deep fascia via a 5–0 absorbable PLA suture. Mouse skins were closed by interrupted sutures and routine feeding condition was applied after mice recovered from anesthetization.

At 7, 28, and 56 d after surgery, animals were euthanized, the implants and surrounding tissues were removed, and a portion was fixed with 4% paraformaldehyde and embedded in paraffin. The tissue sections were stained with hematoxylin and eosin (H&E) and Masson's trichrome. The density and area of giant foreign body cells (FBGCs) within membranes were calculated based on H&E staining images. The thickness of fibrous capsule was measured from Masson's Trichrome staining images with Image J. The other part was undergone qRT PCR analysis. The gene primer sequences are shown in table 1. The M1 and M2 subtypes of macrophages were evaluated by anti-CD86 (1:200 dilution, Bioss) and anti-CD163 (1:200 dilution, Bioss) immunohistochemical staining after 28 and 56 d.

2.8. Statistical analysis

Data are presented as mean ± standard deviation. Statistical analysis was analyzed by one-way or two-way analysis of variance (ANOVA) with Tukey's post hoc multiple comparisons, where appropriate. A p-value less than 0.05 was considered statistically significant.

3. Results

3.1. Physicochemical properties of membranes

The SEM images show that the structure and morphology of electrospun membranes in each group were similar (figure 1(A)). No significant difference in texture, density, and orientation could be visually observed among these fibers. Further FTIR assay showed similar spectra for these fibers which share the same absorbance peaks at 1755 cm^{-1} (symbols of C=O bond), indicating the ester group of PLA backbone (figure 1(B)). We used EDC/NHS to graft the PLA/Gel membrane with CS-IBU conjugate in an MES buffered solution at a low concentration of 1 mg ml^{-1} solution. This process not only chemically coupled PLA/Gel fibers with CS-IBU conjugate but also crosslinked PLA/Gel fibers to increase their stability. The absorbance peaks at 1652 cm^{-1} and 1532 cm^{-1} confirmed the existence of gelatin after prolonged EDC/NHS treatment for 24 h (figure S2).

Fiber diameters in each group typically conformed to a normal distribution, but the fiber diameters of PLA/Gel-CS and PLA/Gel-CS-IBU membranes were slightly higher than those of PLA/Gel membrane (figure 1(C), $p < 0.05$). No significant difference in fiber diameter of PLA/Gel-CS and PLA/Gel-CS-IBU membranes could be detected ($p > 0.05$). There was no significant difference between the groups for UTS and strain at failure, however, the Young's modulus was significantly lower in PLA/Gel-CS group and the difference was significant (figure 1(D), $p < 0.05$).

There were no significant differences in the rate of *in vitro* fiber degradation (demonstrated by weight loss) between all membranes. At week 6, fiber weight loss was approximately 20% in all membranes (figure 1(E), $p > 0.05$). PLA and gelatin degraded with time, accompanied by CS and CS-IBU shedding from fibers. In addition, ibuprofen was gradually released as PLA/Gel-CS-IBU membrane degraded. At day 1, only a small amount of IBU was released, and the cumulative release concentration of IBU over 4 d was approximately 31 μg ml^{-1}. After 28 d, the cumulative release concentration of IBU was approximately 113 μg ml^{-1} (figure 1(F)).

3.2. Antibacterial properties of modified nanofiber membranes

To further validate the anti-bacterial function of modified fiber membranes, the bacterial solution was cultured with each group of membranes respectively. As illustrated in figure 2, the colony density of *E. coli* and *S. aureus* in the PLA/Gel group did not differ significantly from that of the TCP group ($p > 0.05$). In contrast, the colony densities of *E. coli* and *S. aureus* in the PLA/Gel-CS and PLA/Gel-CS-IBU groups were significantly lower than those in the unmodified and TCP groups ($p < 0.05$). However, there was no significant difference in colony density between the PLA/Gel-CS and PLA/Gel-CS-IBU groups ($p > 0.05$).

3.3. Biocompatibility of electrospun membranes

The cytocompatibility of electrospun membranes was evaluated by RAW 264.7 macrophages. Cells proliferated steadily on all membranes, with no significant differences in cell viability or proliferation rates observed. Only a slightly lower cell viability was observed on the first day on the surface of PLA/Gel-CS membrane (figures 3(A) and (C), $p < 0.05$). SEM images reveal that macrophages were firmly attached to the fibers, expanded along the direction of the fibers, and evenly spread on the membrane surface (figure 3(B)). The results above suggest that CS and IBU on the membrane surface did not have a significant effect on macrophage proliferation.

3.4. *In vitro* anti-inflammatory activity

The anti-inflammatory activity of membranes was evaluated by simulating the inflammatory environment *in vitro*. M1-type polarization of macrophages was induced by LPS, there was a significant difference in the M2/M1 ratio of macrophages in response to LPS stimulation. The Flow cytometry analysis indicated that LPS stimulation significantly increased macrophage surface CD86 expression, leading to a significant decrease in the M2/M1 ratio (figures 4(A) and (B), $p < 0.05$). The M2/M1 ratio on PLA/Gel-CS membrane surface decreased further compared to that of PLA/Gel, but then rebounded significantly in PLA/Gel-CS-IBU membrane to reach a level close to that of the control group ($p < 0.05$). On the other hand, nitric oxide release was significantly elevated by LPS stimulation and then reduced in PLA/Gel-CS-IBU group (figure 4(C), $p < 0.05$). Likewise, the elevated ROS synthesis level led by LPS stimulation was largely inhibited on the surface of PLA/Gel-CS-IBU membrane (figure 4(D)).

3.5. Histological analysis

To investigate the extent to which fibrous material inhibits the foreign body reaction by releasing ibuprofen *in vivo*, we analyzed the histological structure of subcutaneously embedded electrospun membranes using H&E and Masson's trichrome staining. As illustrated in figure 5, host cells were recruited to the membranes and gradually infiltrated into their inner part. FBR could be observed in all membranes on

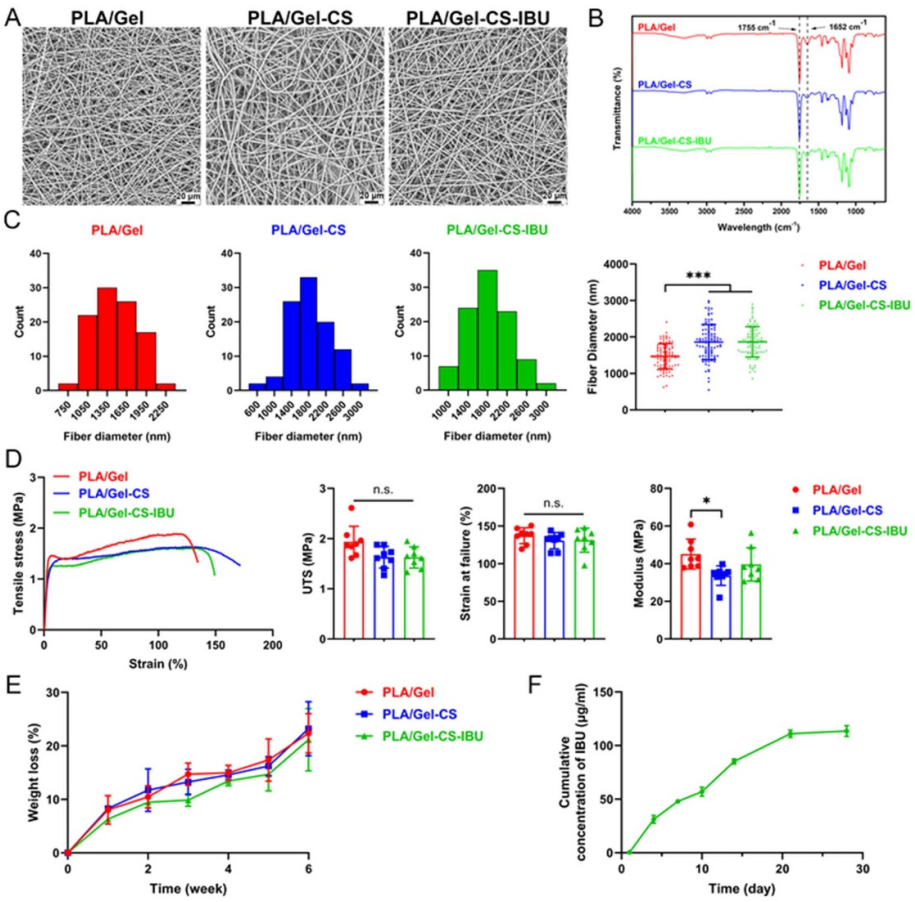

Figure 1. Physicochemical properties of electrospun membranes. SEM images (A), FTIR (B), fiber diameter, uniaxial tensile test (D), drug release (E), and *in vitro* degradation (F) of electrospun membranes. One-way ANOVA with Tukey's post hoc test, * indicates $p < 0.05$, *** indicates $p < 0.001$, n.s. denotes not significant.

day 7 after implantation. FBR was most severe in the PLA/Gel-CS, as indicated by the fastest rate of inflammatory cell infiltration and most FBGC formation compared to the other groups (figures 5(A)–(C), $p < 0.05$). Meanwhile, PLA/Gel-CS membrane degraded the fastest *in vivo*, in contrast to PLA/Gel and PLA/Gel-CS-IBU membranes, which were not completely degraded by day 56. Over time, FBGC infiltrated the entire membrane in PLA/Gel and PLA/Gel-CS groups, leading to the loss of the original fibrous structure by day 56. In contrast, FBGC infiltration in PLA/Gel-CS-IBU group was slower, and the original fibrous architecture remained intact. There was no statistically significant difference in the level of material-induced FBR between PLA/Gel and PLA/Gel-CS-IBU groups (figure 5(D), $p > 0.05$). The thinnest fibrous capsule was formed in PLA/Gel-CS-IBU group on day 28 after subcutaneous implantation (figures 5(B) and (E), $p < 0.05$). However, by day 56, there was no significant difference in the thickness of the fibrous capsule between all groups.

PCR assays of tissue samples show that the phenotype of host macrophages infiltrating membranes differed between the groups. CD86 expression was significantly lower in the PLA/Gel-CS-IBU group than in the PLA/Gel group at day 7, indicating early inhibition of macrophage differentiation towards M1 (figure 6(A), $p < 0.05$). In contrast, at day 56, CD163 expression was significantly higher in the PLA/Gel-CS-IBU group than in the PLA/Gel group, indicating a dominance of M2 subtype macrophages at this time (figure 6(B), $p < 0.05$). However, there was a lack of variability in the expression of the various representative inflammatory factors, with only slightly higher expression of *Il1b* in the PLA/Gel-CS group than in the PLA/Gel group at day 28 (figures 6(C)–(F), $p < 0.05$).

CD86 immunostaining images show that PLA/Gel and PLA/Gel-CS membranes induced more infiltration of M1 subtype macrophages than PLA/Gel-CS-IBU membrane after 28 d. After 56 d, the same differences were still observed. However, CD163 immunostaining images do not show significant differences (figure 7).

4. Discussion

Electrospun membranes are commonly used for tissue regeneration or trauma repair [34–37]. Biodegradable aliphatic polyesters such as PLA and

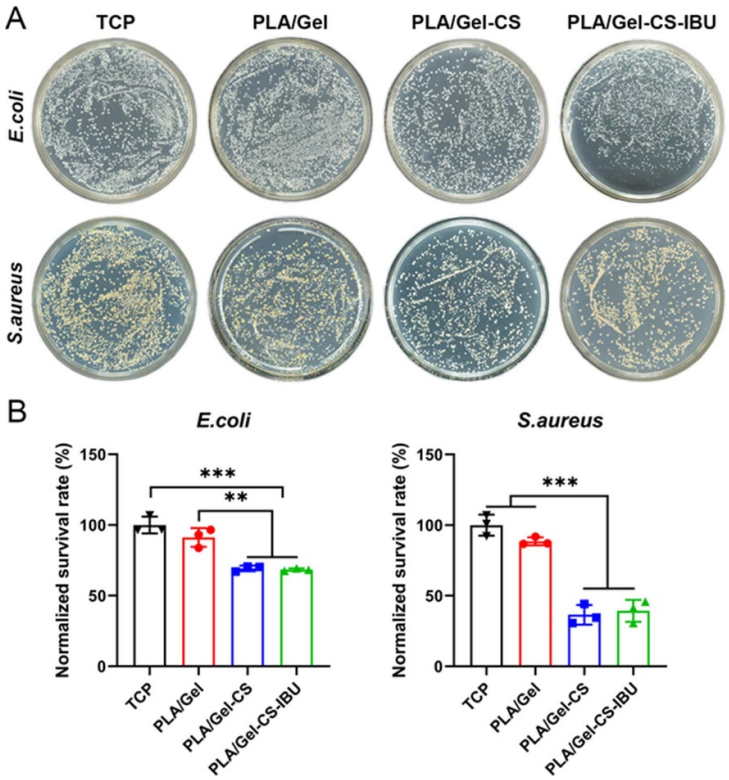

Figure 2. Antibacterial properties of electrospun membranes. Antibacterial macroscopic pictures (A) show *E. coli* and *S. aureus* colonies grown on broth agar plates after treatment with electrospun membranes. Quantitative analysis of *E. coli* and *S. aureus* (B). One-way ANOVA with Tukey's post hoc test, $n = 3$, ** indicates $p < 0.01$, *** indicates $p < 0.001$.

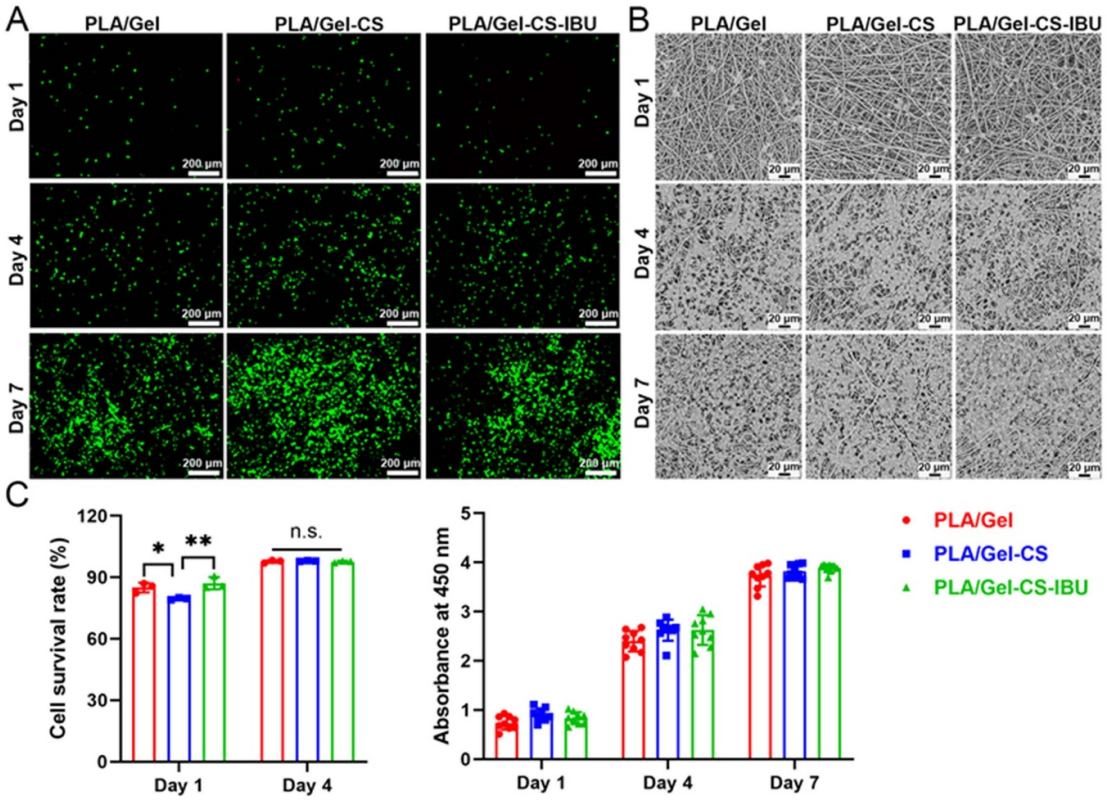

Figure 3. Evaluation of the cytocompatibility of electrospun membranes with RAW 264.7 macrophages. Live/dead staining images (A), SEM images (B), and CCK-8 assay (C) of membranes. Two-way ANOVA with Tukey's post hoc test, * indicates $p < 0.05$, ** indicates $p < 0.01$, n.s. denotes not significant.

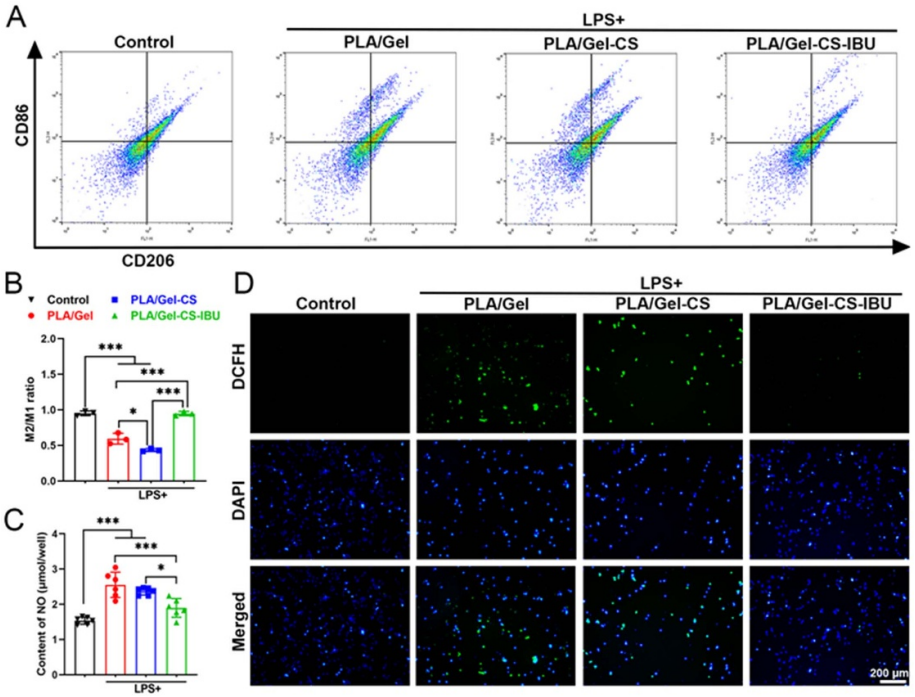

Figure 4. Evaluation of *in vitro* anti-inflammatory activity of electrospun membranes. Flow cytometry analysis shows that PLA/Gel-CS-IBU nanofiber membranes induced a higher M2/M1 macrophage ratio (A)–(B). Levels of NO (C) and ROS (D) of macrophages on electrospun membranes. One-way ANOVA with Tukey's post hoc test, * indicates $p < 0.05$, *** indicates $p < 0.001$.

polyglycolide acid (PGA) are representative materials commonly used in tissue engineering and regenerative medicine. However, their acidic degradation products after implantation can trigger foreign body reactions and localized aseptic inflammation *in vivo*, leading to tissue repair failure or excessive scar formation [14]. It is necessary to rationally modify the surface of basic electrospun membranes to enhance their histocompatibility. Gelatin is a product of collagen hydrolysis, rich in amino and carboxyl groups, which can react with the amino groups of chitosan [4, 38]. Macrophage polarization at the implantation site is the central element mediating the generation of aseptic inflammation and FBR [17, 21]. Therefore, in this study, by coating chitosan and ibuprofen on the fiber surface, we fabricated electrospun fiber membranes to modulate macrophage phenotype and accelerate macrophage polarization towards the M2 direction without affecting cytocompatibility, which aims at achieving the alleviation of post-implantation FBR.

The modified electrospun membranes were preliminarily characterized morphologically and physiochemically, indicating that their properties are essentially the same as those of the unmodified membranes. However, the fibers coated with chitosan had larger diameters, but their elasticity was slightly reduced. In our previous study, the introduction of CS, which is considered an inelastic component, is likely related to the weakening of elasticity in the modified electrospun membranes [14, 39]. The new amide bond formed between CS and IBU was not observed in FITR, as the grafting amount of CS-IBU was relatively low. In our earlier study, we used a relatively higher concentration of ∼3 mg ml^{-1} CS-IBU to graft with PLA/Gel fibers, it had enriched content, so new amide bonds could be observed in FITR (unpublished data). In addition, the presence of IBU was detected by drug release experiments, confirming that CS-IBU has been grafted onto the electrospun membrane.

Chitosan is the product of chitin after deacetylation reaction and has excellent antibacterial ability, which is primarily determined by the free amino groups ($–NH_2$). In addition, its antibacterial properties are also affected by its degree of deacetylation (DD), molecular weight and the physicochemical properties of C2–NH_2, C3–OH (secondary hydroxyl), and C6–OH (primary hydroxyl) functional groups [40, 41]. We found that after modification, PLA/Gel-CS and PLA/Gel-CS-IBU membranes exhibited certain antibacterial properties (figure 2). At the same time, our results show that there was no significant difference in the antibacterial effect of PLA/Gel-CS and PLA/Gel-CS-IBU membranes. This may be because even though the amidation reaction between CS and IBU leads to a decrease in the number of amino groups ($–NH_2$) on CS, the limited grafting of CS and CS-IBU due to the dense fiber structure of the membrane itself does not have a significant effect

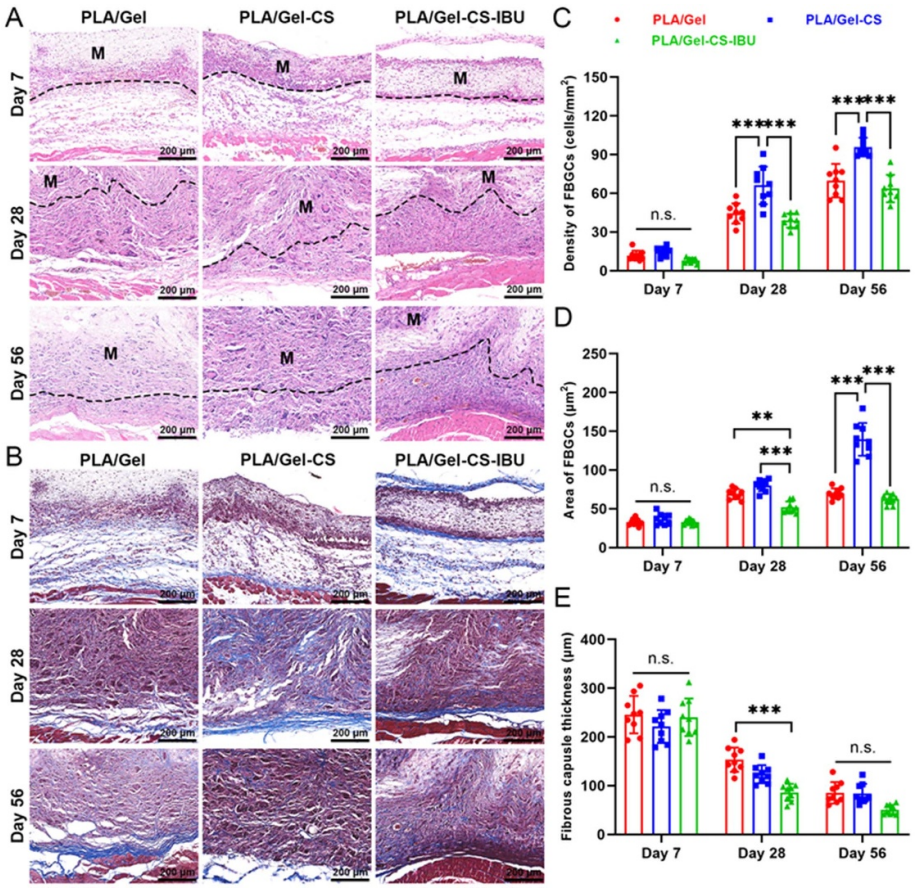

Figure 5. Histological analyses of host response to electrospun membranes. H&E (A) and Masson's trichrome staining (B) of retrieved membranes at days 7, 28, and 56. M stands for membranes. The density of FBGCs (C) and the area of FBGCs (D) are measured from H&E staining images, and the thickness of fibrous capsule (E) is measured from the Masson trichrome staining images. Two-way ANOVA with Tukey's post hoc test, $n = 9$ for C, D, and E, ** indicates $p < 0.01$, *** indicates $p < 0.001$, n.s. denotes not significant.

on the reduction of amino groups. Similar findings were reported in our previous study where no significant difference in antibacterial activity between electrospun membranes grafted with CS and CS–OI was found [29].

We evaluated the cell compatibility of the modified membrane. Our results indicate that both PLA/Gel-CS and PLA/Gel-CS-IBU membranes exhibit good cell compatibility (figure 3). Ibuprofen show negligible cytotoxicity at low concentrations, but when the concentration exceeds 15 μg ml^{-1}, it will produce cytotoxicity [42]. In this study, PLA/Gel-CS-IBU membrane was able to achieve sustained release of IBU, avoiding cytotoxicity caused by sudden release of IBU (figure 1(F)).

The FBR generated after material implantation will have adverse effects on the integration between the material and the host, resulting in implant failure [18]. Activation of macrophages is the key event that triggers the FBR to the implant. Therefore, the regulation of macrophage phenotype and its mediated inflammation is also one of the means to promote tissue remodeling and wound healing [43]. Results show that LPS activated the expression of CD86 on the surface of macrophages and promoted the transformation of macrophages to M1 phenotype under conditions simulating inflammation *in vitro*, resulting in a significant decrease in M2/M1 ratio, but PLA/Gel-CS-IBU membrane could increase M2/M1 ratio (figures 4(A) and (B)). However, this did not fully indicate that PLA/Gel-CS-IBU membrane can promote the transformation of macrophages to M2 phenotype. Therefore, *in vivo* studies on all membranes were conducted. The CD86 expression of PLA/Gel-CS-IBU membrane was low at the initial stage of material implantation *in vivo*, indicating that PLA/Gel-CS-IBU membrane inhibited macrophage differentiation into M1 in the early stage (figure 6(A)). However, after a period of time, PLA/Gel-CS-IBU membrane promoted the expression of CD163, indicating that M2 subtype macrophages were dominant at this time (figure 6(B)). The transformation of macrophages from M1 to M2 will help to reduce the FBR implanted by materials and promote the strong integration and beneficial remodeling of biomaterials into host tissues [44].

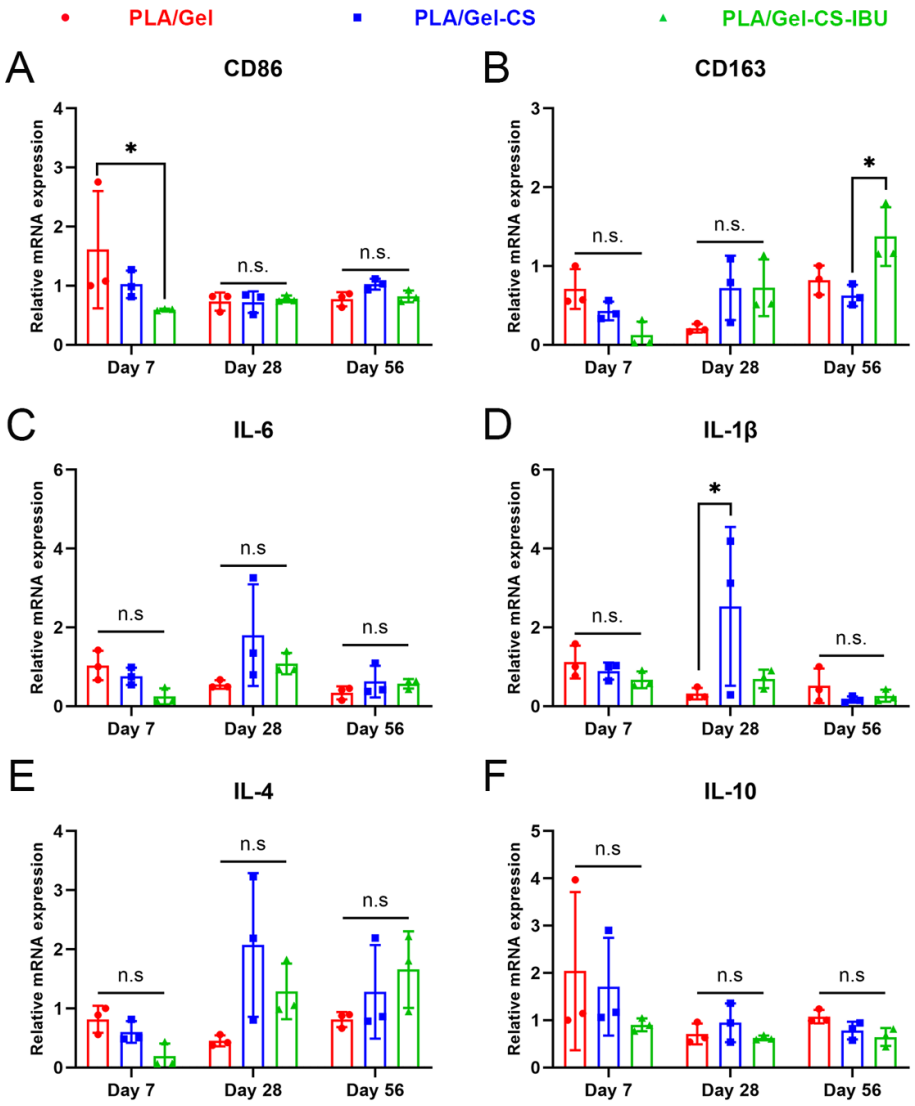

Figure 6. Tissue qRT-PCR assay. The gene expression levels of CD86, CD163, *Il6*, *Il1b*, *Il4*, and *Il10* of tissues (A)–(F). Two-way ANOVA with Tukey's post hoc test, $n = 3$, * indicates $p < 0.05$, n.s. denotes not significant.

The introduction of non-steroidal anti-inflammatory drugs (such as ibuprofen) on the surface of membrane may be an effective measure to alleviate FBR of the electrospun membrane [5, 45, 46]. Dysregulated inflammatory responses lead to ineffective implantation of materials, which is not conducive to wound healing and leads to the formation of scar tissue [47]. As an important part of the immune system, macrophages actively participate in the inflammatory response and promote the repair of tissues during the material implantation process. ROSs generally refers to free radicals and non-free radicals in oxygen sources. It is the product of normal oxygen metabolism, and an appropriate amount of ROS can promote immunity and repair. During the acute inflammatory response, the release of pro-inflammatory factors such as TNF-α and IL-6 promote the mass production of ROS in a short time, and finally effectively remove foreign bodies. However, superfluous ROS will damage inflammatory tissues [48]. IBU exerts antioxidant function by partially activating peroxisome proliferator activated receptor γ [49, 50]. *In vitro* results show that PLA/Gel-CS-IBU membrane could significantly inhibit ROS in macrophages (figure 4(D)). Besides, macrophage-fused FBGCs were observed in all membranes after implantation. After 56 d, fewer FBGCs were observed in the PLA/Gel-CS-IBU membrane than in PLA/Gel-CS (figures 5(A)–(D)). It was also observed that the fibrous capsule formed by the PLA/Gel-CS-IBU membrane was the thinnest at day 28. In addition, regulating the expression of inflammatory factors is also one of the means to reduce inflammation and promote wound healing [51]. Tissue qRT-PCR results show that on day 28, the expression of pro-inflammatory factor *Il1b* in the PLA/Gel-CS group was only slightly higher than that in PLA/Gel group, and there was no significant difference between pro-inflammatory factor *Il6* and anti-inflammatory factors *Il4* and *Il10* in three

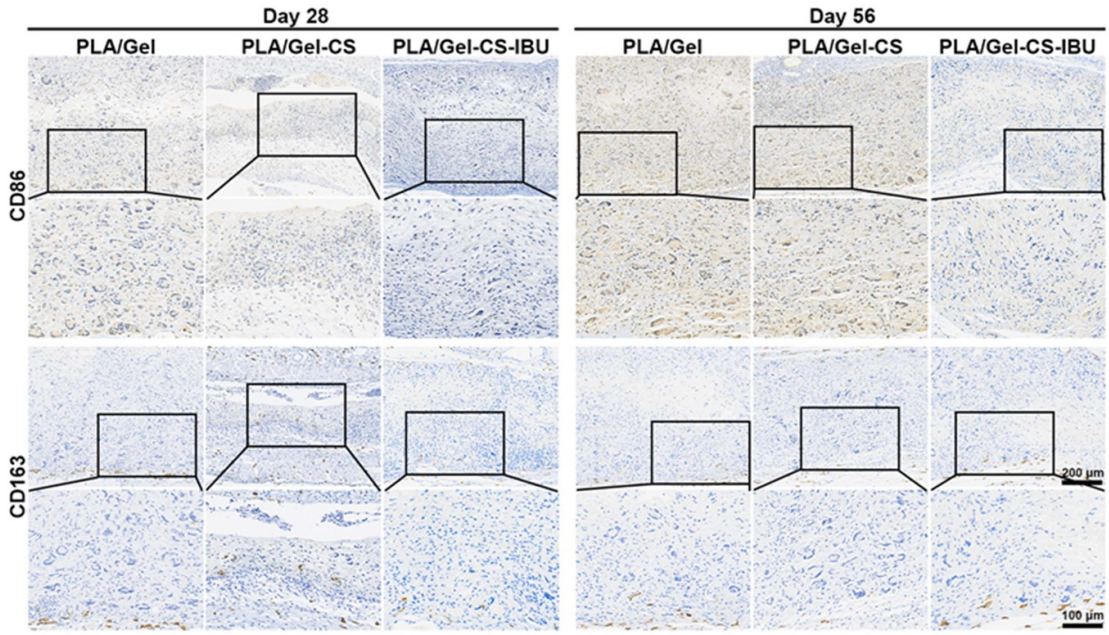

Figure 7. Immunohistochemical analyses of macrophage phenotype.

groups (figure 6). This may be due to individual differences. Therefore, we still need to further study the regulatory role of PLA/Gel-CS-IBU membrane on inflammatory factors by other methods in the future.

5. Conclusions

Electrospun membranes were functionalized with CS and IBU via carbodiimide chemistry. This strategy granted electrospun membranes with good antibacterial and anti-inflammatory activity. The PLA/Gel-CS-IBU membrane showed mitigated inflammatory responses in subcutaneous implantation. This study provides an effective approach to functionalizing electrospun membranes for implantation.

Data availability statement

All data that support the findings of this study are included within the article (and any supplementary files).

Acknowledgment

The authors acknowledge financial support from the National Key R&D Program of China (2021FYC2400800), Natural Science Foundation of Zhejiang Province (LY22C100001), National Natural Science Foundation of China (32071340), Fundamental Research Funds for the Central Universities of Donghua University (2232023D-09), and the Medical Innovation Research Project of Science and Technology Innovation Action Plan of Shanghai Science and Technology Committee 2021 (21Y11908700). This project was also supported by Researchers Supporting Project Number (RSP2025R65), King Saud University, Riyadh, Saudi Arabia.

ORCID iDs

Qiaolin Ma https://orcid.org/0009-0000-0113-8296
Mohamed El-Newehy https://orcid.org/0000-0002-4265-0701
Jinglei Wu https://orcid.org/0000-0001-9549-3992
Tian Tu https://orcid.org/0000-0001-8231-0210

References

[1] Jiang T, Carbone E J, Lo K W H and Laurencin C T 2015 Electrospinning of polymer nanofibers for tissue regeneration *Prog. Polym. Sci.* **46** 1–24
[2] McCarthy A, Avegnon K L M, Holubeck P A, Brown D, Karan A, Sharma N S, John J V, Weihs S, Ley J and Xie J 2021 Electrostatic flocking of salt-treated microfibers and nanofiber yarns for regenerative engineering *Mater. Today Bio.* **12** 100166
[3] Zulkifli M Z A, Nordin D, Shaari N and Kamarudin S K 2023 Overview of electrospinning for tissue engineering applications *Polymers* **15** 2418
[4] Fazal F, Melchels F P W, McCormack A, Silva A F, Handley E L, Mazlan N A, Callanan A, Koutsos V and Radacsi N 2024 Fabrication of a compliant vascular graft using extrusion printing and electrospinning technique *Adv. Mater. Technol.* **9** 2400224
[5] Liu J, Tang R, Zhu X, Ma Q, Mo X, Wu J and Liu Z 2024 Ibuprofen-loaded bilayer electrospun mesh modulates host response toward promoting full-thickness abdominal wall defect repair *J. Biomed. Mater. Res.* A **112** 941–55
[6] Peranidze K, Safronova T V and Kildeeva N R 2023 Electrospun nanomaterials based on cellulose and its

derivatives for cell cultures: recent developments and challenges *Polymers* **15** 1174
[7] Jiménez-Beltrán M A, Gómez-Calderón A J, Quintanar-Zúñiga R E, Santillán-Cortez D, Téllez-González M A, Suárez-Cuenca J A, García S and Mondragón-Terán P 2022 Electrospinning-generated nanofiber scaffolds suitable for integration of primary human circulating endothelial progenitor cells *Polymers* **14** 2448
[8] Chen K, Li Y, Li Y, Pan W and Tan G 2022 Silk fibroin combined with electrospinning as a promising strategy for tissue regeneration *Macromol. Biosci.* **23** 2200380
[9] Yang C, Shao Q, Han Y, Liu Q, He L, Sun Q and Ruan S 2021 Fibers by electrospinning and their emerging applications in bone tissue engineering *Appl. Sci.* **11** 9082
[10] Rostami M *et al* 2023 Recent advances in electrospun protein fibers/nanofibers for the food and biomedical applications *Adv. Colloid Interface Sci.* **311** 102827
[11] Agarwal A, Rao G K, Majumder S, Shandilya M, Rawat V, Purwar R, Verma M and Srivastava C M 2022 Natural protein-based electrospun nanofibers for advanced healthcare applications: progress and challenges *3 Biotech* **12** 92
[12] Khadka D B and Haynie D T 2012 Protein- and peptide-based electrospun nanofibers in medical biomaterials *Nanomed. Nanotechnol. Biol. Med.* **8** 1242–62
[13] Ghafouri S, Sadeghi-avalshahr A R, Molavi A M and Hassanzadeh H 2022 Fabrication of functionally graded electrospun membranes based on silk fibroin for using as dental barrier membranes in guided bone regeneration *Fibers Polym.* **23** 2549–56
[14] Shen Y, Tu T, Yi B, Wang X, Tang H, Liu W and Zhang Y 2019 Electrospun acid-neutralizing fibers for the amelioration of inflammatory response *Acta Biomater.* **97** 200–15
[15] Cramer M, Chang J, Li H, Serrero A, El-Kurdi M, Cox M, Schoen F J and Badylak S F 2021 Tissue response, macrophage phenotype, and intrinsic calcification induced by cardiovascular biomaterials: can clinical regenerative potential be predicted in a rat subcutaneous implant model? *J. Biomed. Mater. Res.* A **110** 245–56
[16] Wei F *et al* 2021 Host response to biomaterials for cartilage tissue engineering: key to remodeling *Front. Bioeng. Biotechnol.* **9** 664592
[17] Chu C, Liu L, Rung S, Wang Y, Ma Y, Hu C, Zhao X, Man Y and Qu Y 2019 Modulation of foreign body reaction and macrophage phenotypes concerning microenvironment *J. Biomed. Mater. Res.* A **108** 127–35
[18] Gibon E, Takakubo Y, Zwingenberger S, Gallo J, Takagi M and Goodman S B 2024 Friend or foe? Inflammation and the foreign body response to orthopedic biomaterials *J. Biomed. Mater. Res.* A **112** 1172–87
[19] Cai F, Wang P, Chen W, Zhao R and Liu Y 2023 The physiological phenomenon and regulation of macrophage polarization in diabetic wound *Mol. Biol. Rep.* **50** 9469–77
[20] Sussman E M, Halpin M C, Muster J, Moon R T and Ratner B D 2013 Porous implants modulate healing and induce shifts in local macrophage polarization in the foreign body reaction *Ann. Biomed. Eng.* **42** 1508–16
[21] Li R, Feng D, Han S, Zhai X, Yu X, Fu Y and Jin F 2023 Macrophages and fibroblasts in foreign body reactions: how mechanical cues drive cell functions? *Mater. Today Bio.* **22** 100783
[22] Martin K E and García A J 2021 Macrophage phenotypes in tissue repair and the foreign body response: implications for biomaterial-based regenerative medicine strategies *Acta Biomater.* **133** 4–16
[23] Gordon S and Martinez F O 2010 Alternative activation of macrophages: mechanism and functions *Immunity* **32** 593–604
[24] You C, Zhu Z, Wang S, Wang X, Han C and Shao H 2023 Nanosilver alleviates foreign body reaction and facilitates wound repair by regulating macrophage polarization *J. Zhejiang Univ. Sci.* B **24** 510–23
[25] Funes S C, Rios M, Escobar-Vera J and Kalergis A M 2018 Implications of macrophage polarization in autoimmunity *Immunology* **154** 186–95
[26] Jin S *et al* 2024 M2 macrophage-derived exosome-functionalized topological scaffolds regulate the foreign body response and the coupling of angio/osteoclasto/osteogenesis *Acta Biomater.* **177** 91–106
[27] Toita R, Kang J-H and Tsuchiya A 2022 Phosphatidylserine liposome multilayers mediate the m1-to-m2 macrophage polarization to enhance bone tissue regeneration *Acta Biomater.* **154** 583–96
[28] Pereira A K D S, Reis D T, Barbosa K M, Scheidt G N, da Costa L S and Santos L S S 2020 Antibacterial effects and ibuprofen release potential using chitosan microspheres loaded with silver nanoparticles *Carbohydrate Res.* **488** 107891
[29] He J, Zhou S, Wang J, Sun B, Ni D, Wu J and Peng X 2024 Anti-inflammatory and anti-oxidative electrospun nanofiber membrane promotes diabetic wound healing via macrophage modulation *J. Nanobiotechnol.* **22** 116
[30] Guan X, Yao H and Wu J 2024 Photocrosslinkable hydrogel of ibuprofen-chitosan methacrylate modulates inflammatory response *J. Biomed. Mater. Res.* A **112** 2001–17
[31] Zhang S, Ye J, Sun Y, Kang J, Liu J, Wang Y, Li Y, Zhang L and Ning G 2020 Electrospun fibrous mat based on silver (i) metal-organic frameworks-polylactic acid for bacterial killing and antibiotic-free wound dressing *Chem. Eng. J.* **390** 124523
[32] Yan D, Zhang S, Yu F, Gong D, Lin J, Yao Q and Fu Y 2021 Insight into levofloxacin loaded biocompatible electrospun scaffolds for their potential as conjunctival substitutes *Carbohydrate Polym.* **269** 118341
[33] Liu X, He X, Jin D, Wu S, Wang H, Yin M, Aldalbahi A, El-Newehy M, Mo X and Wu J 2020 A biodegradable multifunctional nanofibrous membrane for periodontal tissue regeneration *Acta Biomater.* **108** 207–22
[34] Mahdipour E and Mequanint K 2022 Films, gels and electrospun fibers from serum albumin globular protein for medical device coating, biomolecule delivery and regenerative engineering *Pharmaceutics* **14** 2306
[35] Mirhaj M, Varshosaz J, Labbaf S, Emadi R, Marcus Seifalian A and Sharifianjazi F 2023 An antibacterial multi-layered scaffold fabricated by 3D printing and electrospinning methodologies for skin tissue regeneration *Int. J. Pharm.* **645** 123357
[36] Li M, Hu M, Zeng H, Yang B, Zhang Y, Li Z, Lu L and Ming Y 2021 Multifunctional zinc oxide/silver bimetallic nanomaterial-loaded nanofibers for enhanced tissue regeneration and wound healing *J. Biomed. Nanotechnol.* **17** 1840–9
[37] Ghosh S, Haldar S, Gupta S, Chauhan S, Mago V, Roy P and Lahiri D 2022 Single unit functionally graded bioresorbable electrospun scaffold for scar-free full-thickness skin wound healing *Biomater. Adv.* **139** 212980
[38] Larue L, Michely L, Grande D and Belbekhouche S 2024 Design of collagen and gelatin-based electrospun fibers for biomedical purposes: an overview *ACS Biomater. Sci. Eng.* **10** 5537–49
[39] Tu T, Shen Y, Wang X, Zhang W, Zhou G, Zhang Y, Wang W and Liu W 2020 Tendon ecm modified bioactive electrospun fibers promote MSC tenogenic differentiation and tendon regeneration *Appl. Mater. Today* **18** 100495
[40] Ke C-L, Deng F-S, Chuang C-Y and Lin C-H 2021 Antimicrobial actions and applications of chitosan *Polymers* **13** 904
[41] Li J, Fu J, Tian X, Hua T, Poon T, Koo M and Chan W 2022 Characteristics of chitosan fiber and their effects towards improvement of antibacterial activity *Carbohydrate Polym.* **280** 119031
[42] Schnell S, Kawano A, Porte C, Lee L E J and Bols N C 2008 Effects of ibuprofen on the viability and proliferation of

rainbow trout liver cell lines and potential problems and interactions in effects assessment *Environ. Toxicol.* **24** 157–65
[43] Hesketh M, Sahin K B, West Z E and Murray R Z 2017 Macrophage phenotypes regulate scar formation and chronic wound healing *Int. J. Mol. Sci.* **18** 1545
[44] Wang Y, Fan Y and Liu H 2021 Macrophage polarization in response to biomaterials for vascularization *Ann. Biomed. Eng.* **49** 1992–2005
[45] Liu S *et al* 2017 Electrospun fibrous membranes featuring sustained release of ibuprofen reduce adhesion and improve neurological function following lumbar laminectomy *J. Control. Release* **264** 1–13
[46] Vacanti N M, Cheng H, Hill P S, Guerreiro J D T, Dang T T, Ma M, Watson S, Hwang N S, Langer R and Anderson D G 2012 Localized delivery of dexamethasone from electrospun fibers reduces the foreign body response *Biomacromolecules* **13** 3031–8
[47] Chen G, Yu Y, Wu X, Wang G, Ren J and Zhao Y 2018 Bioinspired multifunctional hybrid hydrogel promotes wound healing *Adv. Funct. Mater.* **28** 1801386
[48] Yang Z, Min Z and Yu B 2020 Reactive oxygen species and immune regulation *Int. Rev. Immunol.* **39** 292–8
[49] Liu Y-W, Zhu X I A, Cheng Y-Q, Lu Q, Zhang F A N, Guo H A O and Yin X-X 2016 Ibuprofen attenuates nephropathy in streptozotocin-induced diabetic rats *Mol. Med. Rep.* **13** 5326–34
[50] Singh A, Tripathi P and Singh S 2020 Neuroinflammatory responses in Parkinson's disease: relevance of ibuprofen in therapeutics *Inflammopharmacology* **29** 5–14
[51] Liu F, Li X, Wang L, Yan X, Ma D, Liu Z and Liu X 2020 Sesamol incorporated cellulose acetate-zein composite nanofiber membrane: an efficient strategy to accelerate diabetic wound healing *Int. J. Biol. Macromol.* **149** 627–38